Coordinated by Allen Bertagne

Delineation of tectonic features offshore Trinidad using 3-D seismic coherence

Adam Gersztenkorn, Tulsa, Oklahoma, U.S.
John Sharp, BP Amoco, Houston, Texas, U.S.
Kurt Marfurt, Tulsa, Oklahoma, U.S.

Seismic coherence allows interpreters to quickly visualize and map complex fault systems. Calibration to well control adds the ability to recognize important stratigraphic features and potential gas/water contacts. Applying coherence technology to an offshore Trinidad 3-D survey reduced exploration cycle time and improved understanding of tectonic elements in the area. The following shows some ways in which coherence may be used to identify complex fault systems and speed up interpretation.

Accurate coherence analysis requires careful acquisition, process-

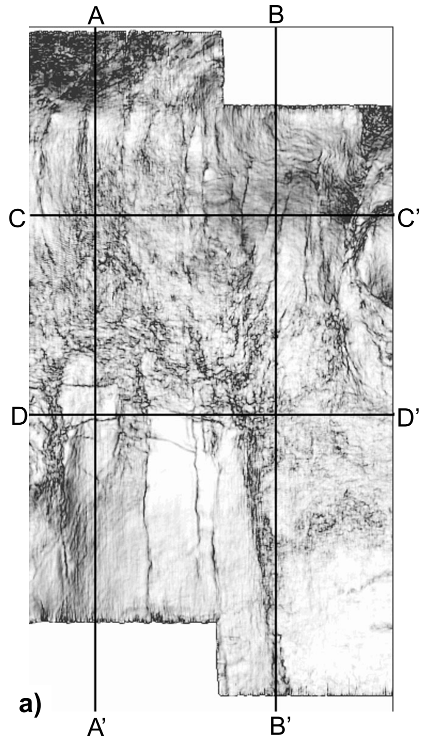

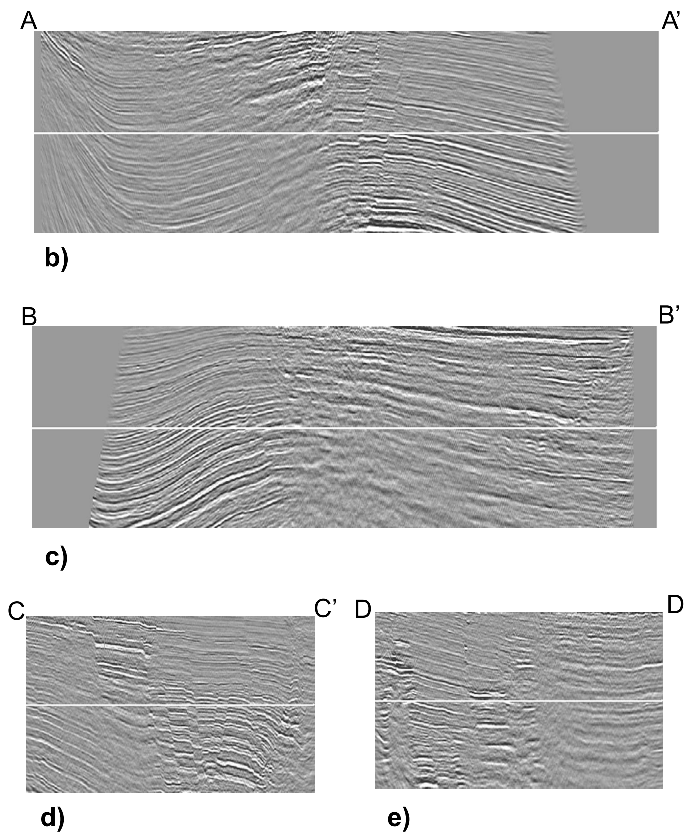

Figure 4. (a) Coherence slice at 1000 ms. Crosshairs indicate cross-sections A-A′, B-B′, C-C′, and D-D′. (b) A-A′ (oriented in direction of compression). Compressional forces at work created anticline, i.e., Galeota Ridge. (c) B-B′. Anticline also depicts the Galeota Ridge, which was formed in response to compressional forces. (d) C-C′ (oriented in direction of extension). Extensional forces cause the drop-down stairstep feature. (e) D-D′ (also oriented along direction of extension) shows resulting faulting.

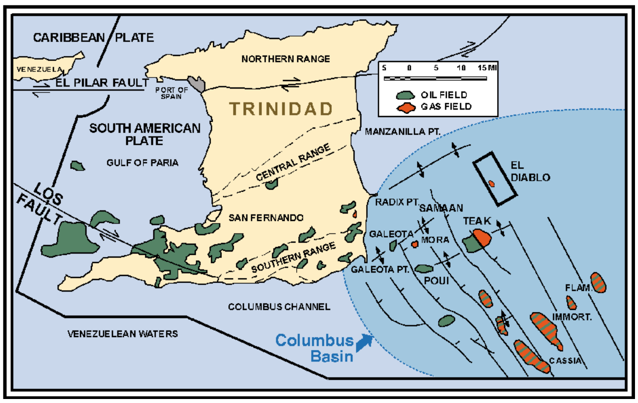

Figure 1. The study area.

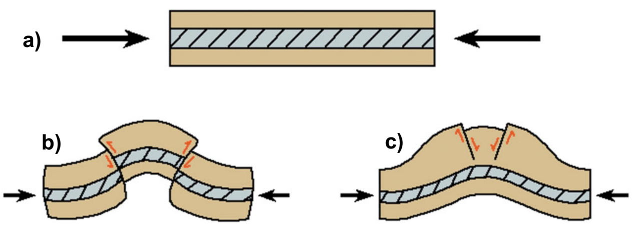

Figure 2. (a) Hypothetical flat-layered model prior to compression oriented parallel to compressional forces (northwest-southeast). (b) Hypothetical pop-up feature due to compression in the model. (c) Hypothetical drop-down feature due to flexure.

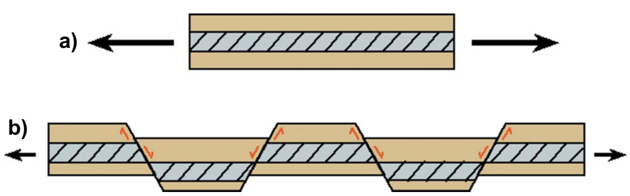

Figure 3. (a) Hypothetical flat-layered model prior to extension oriented parallel to extensional forces (northeast-southwest). (b) Hypothetical horst and graben system resulting from extensional forces.

ing, and time or depth migration of the 3-D volume. Any prior improvement made in sharpness of faults within the migrated 3-D volume directly increases the lateral fault resolution observed on coherence time or depth slices. With accurate velocity models, depth-migrated sections usually result in higher-resolution coherence images than time migrations. The coherence slices in this paper were obtained by applying the eigenstructure-based coherence algorithm to migrated data. Details of this approach are given in Gersztenkorn and Marfurt (1999).

Study area. In early 1992, Amoco acquired a 48-fold, 3-D seismic survey over approximately 112 km^2. Prior to the coherence computations, the 3-D volume was depth migrated and then converted to time. The survey area (Figure 1) is 40 km off the east coast of Trinidad in 70 m of water just east of Samaan Field. The Galeota Ridge trends northeast-southwest through the area. A series of northwest-southeast extensional faults also bisects the area. Hydrocarbon traps occur where faults intersect the Galeota Ridge.

Figures 2a, 2b, and 2c depict the result of a compressional régime on a hypothetical layered model. Compressional forces, in addition to causing folds and anticlines, sometimes cause pop-up blocks (Figure 2b) and grabens at the top of the folds (Figure 2c). In relationship to the regional map of Figure 1, these compressional forces are oriented northwest-southeast; the smaller-scale faults at the top of the folds run northeast-southwest. The Galeota Ridge was formed in response to the compressional forces associated with the motion of the Caribbean and South American Plates. As expected, the Galeota Ridge is perpendicular to these compressional forces.

Figures 3a and 3b illustrate a hypothetical extensional régime. The horst and graben system (Figure 3b) is typical of such extensional forces. Again, referring to Figure 1, the extensional forces are oriented northeast-southwest. The large-scale regional faults in Figure 1 are a direct result of sediment loading within the Columbus Basin and the associated extensional forces.

Overview. Coherence is a quantitative measure of similarity or continuity between waveforms. In the following figures, darker shades represent low coherence, and lighter shades represent higher coherence. Faults, due to a lack of continuity, therefore appear as dark linear or curved features on coherence slices. Figure 4a, a coherence slice extracted at 1000 ms from a cube of coherence values, shows where four cross-sections (Figures 4b-e) were extracted from the seismic data. Cross-sections A-A′ and B-B′ were extracted parallel to the regional compressional forces; C-C′ and D-D′ were extracted parallel to extensional forces. Visual inspection of the coherence slice indicates that the dark linear features correspond to fault locations on the four cross-sections.

The Galeota Ridge is easily observed on A-A′ and B-B′ as a large

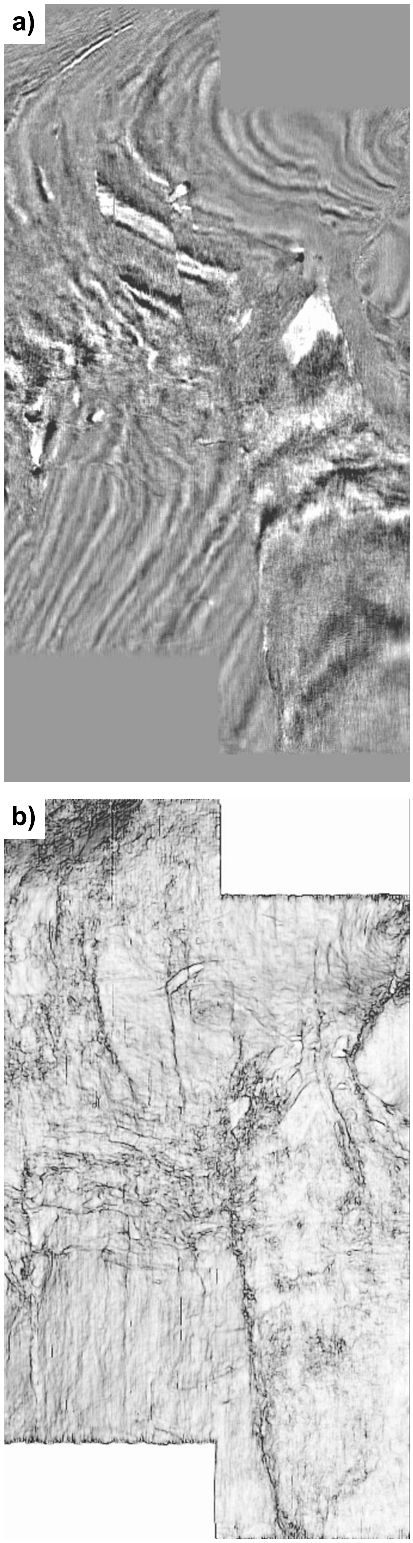

Figure 5. (a) Time slice at 600 ms and (b) corresponding coherence slice at 600 ms.

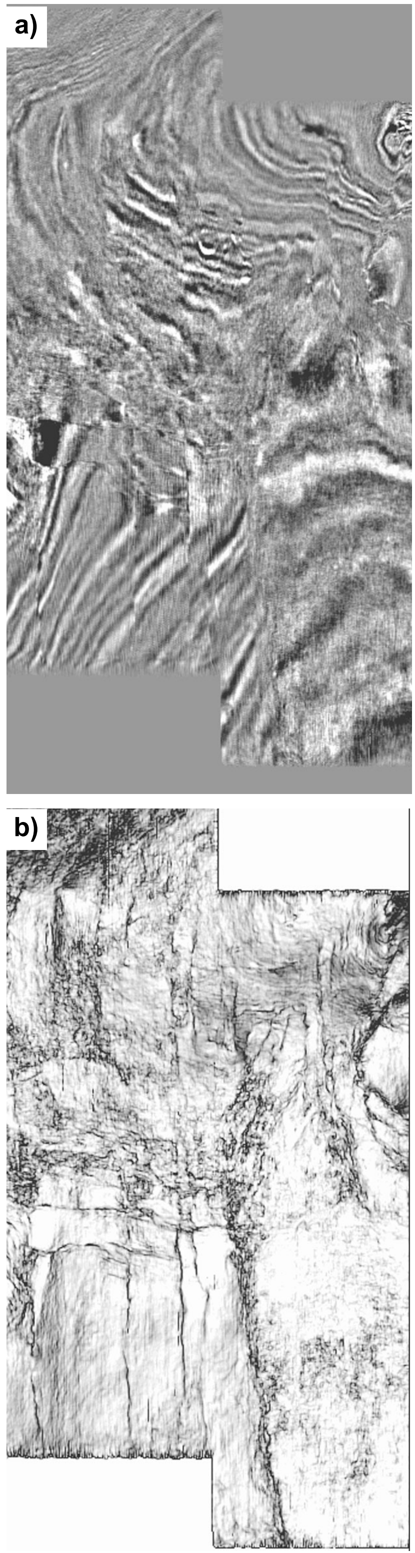

Figure 6. (a) Time slice at 800 ms and (b) corresponding coherence slice at 800 ms.

anticline with more than 750 ms rollover trending northwest-southeast. The apex of the anticlinal features on A-A′ and B-B′ defines the Galeota Ridge. This apex is also where the greatest stress is present due to flexure. The stress at the apex of the anticline induces faulting and in A-A′ a typical drop-down graben feature appears. These faults, which are downthrown to the northwest, have a lateral configuration that is easily observed on the coherence slice at 1000 ms in Figure 4a. B-B′(Figure 4c) shows a similar anticline due to compression. Although the data are not as clean as in A-A′, faulting can be detected close to the apex of the anticline. The decrease in data quality on A-A′ and B-B′ relates to shallow gas in the upper part of the cross-section. Also shown in Figures 4d-e are cross-sections C-C′ and D-D′. In contrast, these cross-sections are oriented parallel to extensional forces and thus parallel to the Galeota Ridge. C-C′ reveals a series of downthrown faults to the northeast in response to extensional forces. D-D′ illustrates similar faulting in the direction of and in response to extension. The coherence slice at 1000 ms in Figure 4a combines the information from all the cross-sections to give a comprehensive view of fault patterns trending in both compressional and

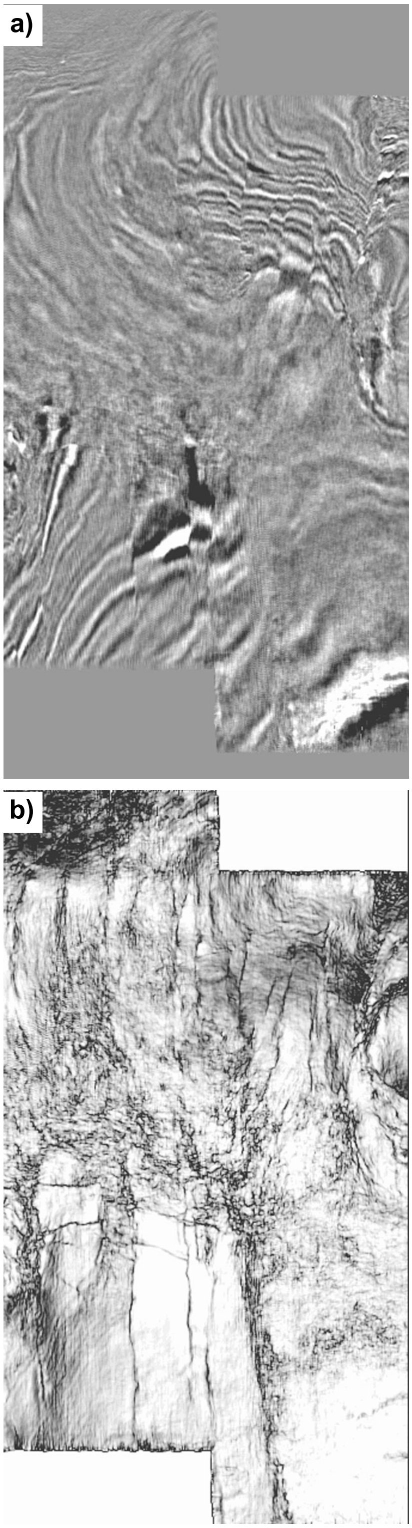

Figure 7. (a) Time slice at 1000 ms and (b) corresponding coherence slice at 1000 ms.

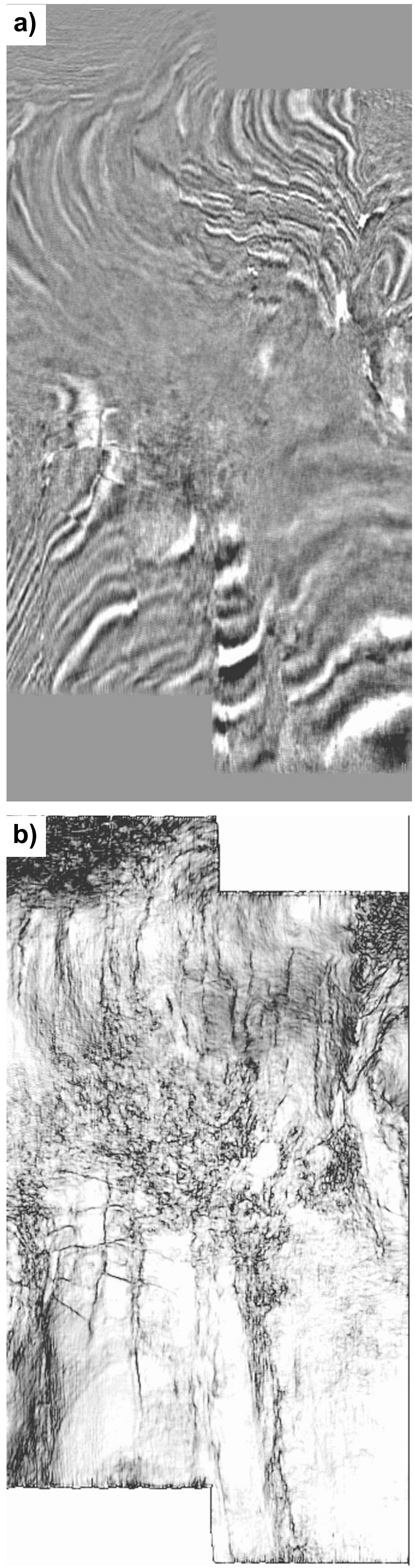

Figure 8. (a) Time slice at 1200 ms and (b) corresponding coherence slice at 1200 ms.

extensional directions.

Figures 5-8 give a cursory view of the entire survey and an overall comparison of coherence and depth-migrated time slices at 600 ms, 800 ms, 1000 ms, and 1200 ms, respectively. In Figures 5a, 6a, 7a, and 8a, the Galeota Ridge can be identified in the upper left of the survey by the wraparound of the reflectors. This typical wraparound indicates that the ridge is dipping from northeast to southwest. On the time slices in the same figures, a structural low is evident just northwest of the ridge. The accompanying coherence slices (Figures 5b, 6b, 7b, and 8b) indicate a series of northwest-southeast faults penetrating through the Galeota Ridge. These are extensional faults that are down-thrown to the northeast. These extensional faults intersect a northeast-southwest set of faults related to the compressional forces that formed the Galeota Ridge. In general, both extensional and compressional faults are much easier to see and interpret on coherence slices than on time slices.

Comparison of the coherence slices at progressively greater depths indicates that fault complexity increases with depth. The individual fault blocks change shape and migrate to the east following the fault plane, also dipping to the east. The coherence slice at 600 ms (Figure 5b) vividly brings out a small channel and associated delta (above the center of the coherence slice) that are not obvious on the migrated time slice. The high amplitudes associated with this small channel on both the migrated and coherence time slices indicate shallow gas accumulations. The time slice at 1200 ms (Figure 8b) shows an area of subdued amplitudes and low coherence values. This zone of low reflectivity in the central portion of the time slice results from the shadowing effect of a shallow gas accumulation.

The previous discussion provides a cursory view of the area. In the following discussion, we focus in greater detail on three regions within the survey and observe their individual structural styles and their manifestations in terms of coherence and dip/azimuth. We point out some interesting features in each region and culminate with region 3, the site of a recently discovered gas field.

Region 1. This region (Figure 9a) covers approximately 5 square miles on the eastern side of the survey. In Figure 9a, a coherence slice is displayed at 800 ms; Figures 9b-d represent magnifications of region 1 at 600, 800, and 1000 ms. The most prominent feature in these figures is an arc-shaped curve delineating a faulted block. As we progress from 600 to 1000 ms on the coherence slices, this arc moves from left to right, indicating that the fault is dipping in the same direction. Comparison of the coherence slices in Figure 9 and the seismic cross-sections in Figures 10c-d reveals this feature is a graben. This area, once considered a prospect, was eventually drilled. Unfortunately, the expected reserves were not found. Proceeding from cross-section A-A′ to cross-section B-

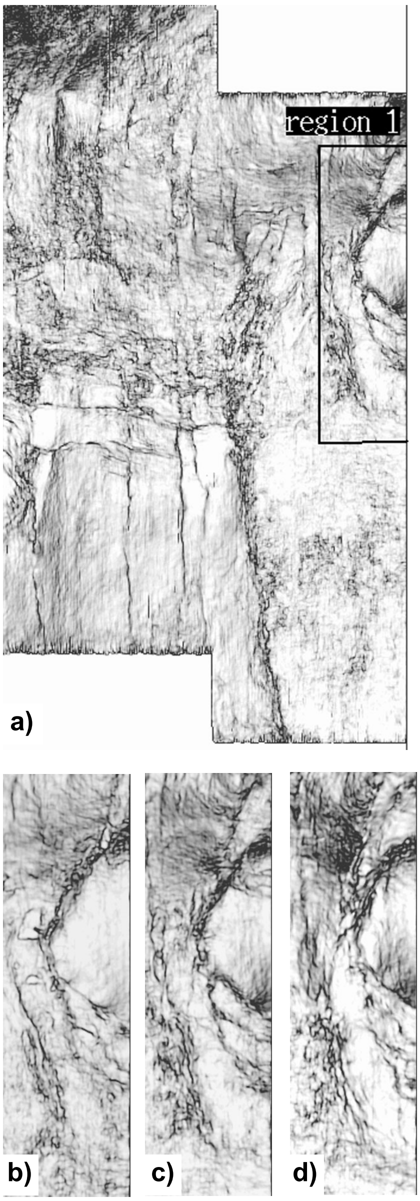

Figure 9. (a) Coherence slice and relative position of region 1 at 800 ms. (b) Region 1 magnified at 600 ms, (c) at 800 ms, and (d) at 1000 ms.

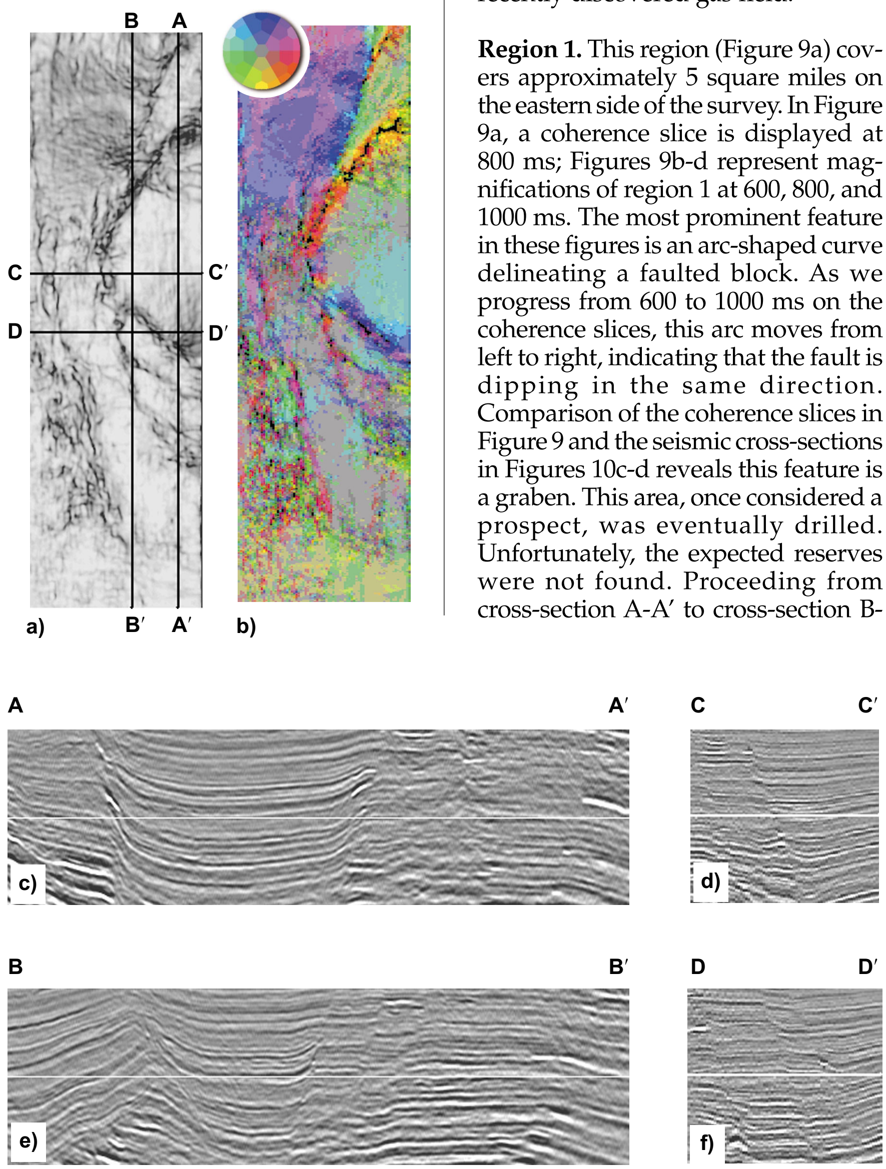

Figure 10. (a) Magnified coherence slice of region 1 at 800 ms with locations of four cross-sections marked. (b) Dip/azimuth slice at 800 ms. (c) A-A′; (d) B-B′; (e) C-C′; and (f) D-D′.

B′ defines the boundaries of the fault block in region 1. C-C′ and D-D′ confirm that the slope of the fault plane moves toward the northeast.

Figure 10b is a dip/azimuth slice generated by the semblance-based coherence algorithm (1998, Marfurt et al.). The colors provide information on direction of maximum dip, or azimuth, and amount of dip. The amount of dip is indicated by the degree of saturation of a specific color on the color wheel. The saturation increases to a maximum on the outside of the color wheel as seen by the very bright colors. Saturation decreases for every color in the direction of the center of the wheel. Zero saturation, represented by gray at the center of the wheel, indicates no dip. The direction of dip on the color wheel is indicated directly by the color itself. The dip/azimuth slice at 800 ms (Figure 10b) displays an apparent scissors-type fault where rotation produced blocks dipping in opposite directions on either side of the fault. Red and magenta in the fault blocks represent dips to the north and northeast; yellow and light green indicate dips to the south and southeast. The large expanse of gray on the dip/azimuth plot associated with the arc-shaped fault in the middle of region 1 suggests very little dip associated with the reflectors.

Region 2. In Figure 11a, the coherence slice at 1100 ms, shows the relative location of region 2. This region encloses approximately 9 square miles on the northeastern part of the 3-D survey. The magnified display of region 2 shows a series of, more or less, northwest-southeast faults. Extensional forces oriented roughly northeast-southwest are responsible for these fault trends.

Figures 11c-d provide two orthogonal cross-sectional views through region 2. Cross section A-A′ runs parallel to the faults and shows the northern flank of the Galeota Ridge, which clearly results from compressional forces. On the other hand, cross-section B-B′ reveals a series of faulted blocks on the flank of the Galeota Ridge caused by extensional forces. The two cross-sections suggest that the geologic history of the area is complex with both compressional and extensional forces shaping the current structure. The dip/azimuth plot in Figure 11e indicates that dips increase in an easterly direction (as evidenced by the brightening of the red and magenta colors), with maximum dips observed along the northwest-southeast fault on the eastern side of region 2. The reflectors dip in a north-northeasterly direction. We confirm this on B-B′ where the dip rate increases near the right edge of the cross-section at 1100 ms.

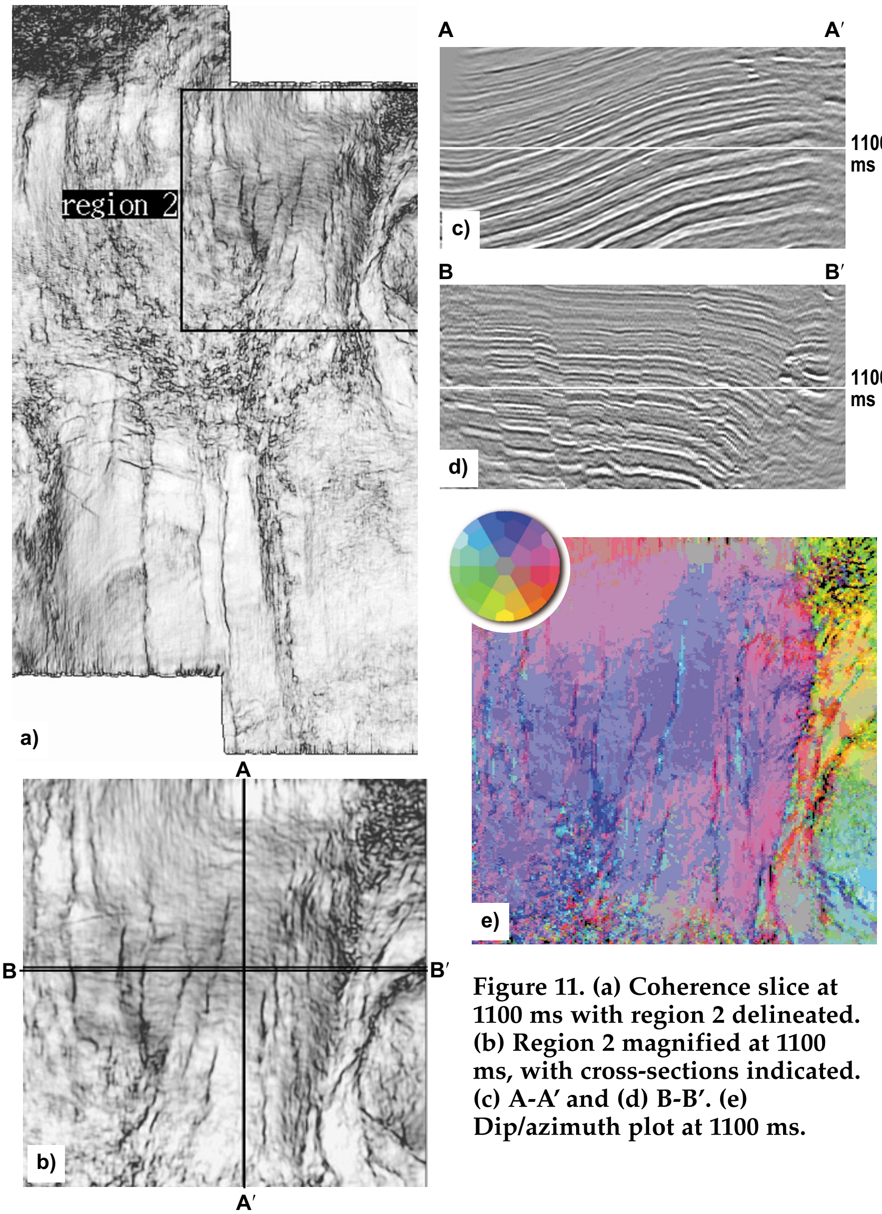

Figure 11. (a) Coherence slice at 1100 ms with region 2 delineated. (b) Region 2 magnified at 1100 ms, with cross-sections indicated. (c) A-A′ and (d) B-B′. (e) Dip/azimuth plot at 1100 ms.

Region 3. Figure 12a locates region 3 in relationship to the entire survey. This region, approximately 9 square miles, is on the west of the survey—a region of particular interest because it includes a recently drilled well and contains a gas field with reserves estimated at 1.1 trillion ft^3.

Gas accumulations in the area display bright amplitudes and occur at the intersection of orthogonal fault trends. The relationship between amplitude and coherence allows interpreters to quickly screen a series of 3-D coherence time slices and identify potential gas accumulations at the intersects of faults. The actual gas accumulation manifests itself on a coherence time slice as a high-coherence response; faults show up as a linear zone of low coherence. This time-slice information was used to plan out a mapping strategy that focused on the area of strong coherence response. Detailed mapping and subsequent attribute analysis of several coherence indicators verified the presence of several stacked gas accumulations that were later successfully drilled. The structural culmination of the Galeota Ridge is the approximate location of the 1995 discovery well.

The coherence slice in Figure 12d, a magnification of the region at 1200 ms, reveals a complex network of faults in orthogonal directions. The throw across the northwest-southeast faults is down to the northeast. The intersecting northeast-southwest faults predominantly dip down to the north,

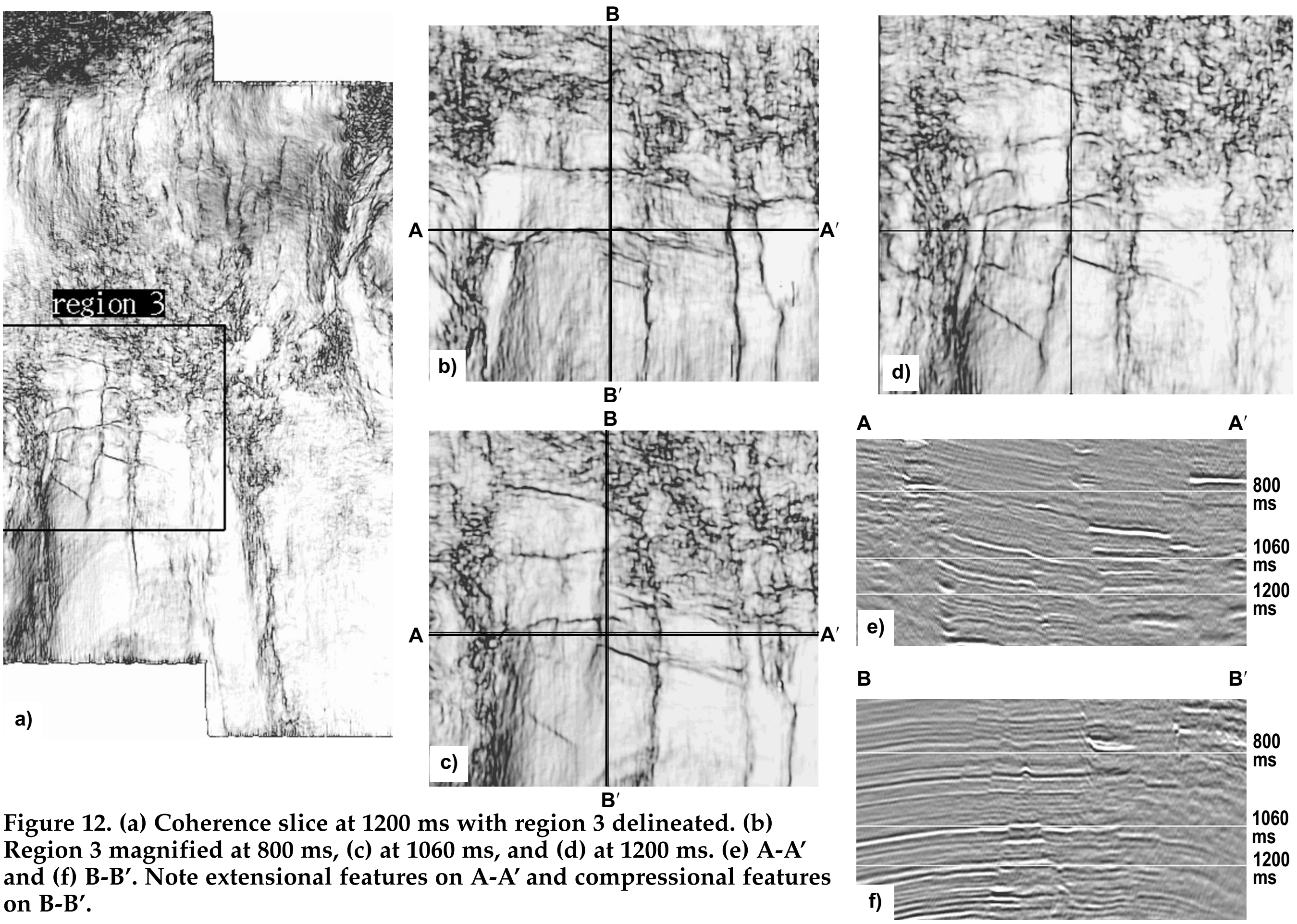

Figure 12. (a) Coherence slice at 1200 ms with region 3 delineated. (b) Region 3 magnified at 800 ms, (c) at 1060 ms, and (d) at 1200 ms. (e) A-A′ and (f) B-B′. Note extensional features on A-A′ and compressional features on B-B′.

with several of these faults demonstrating throw in the opposite direction. Figures 12b-c portray region 3 at 800 ms and 1060 ms, respectively. These figures show that faulting complexity increases with depth through the shallow part. The high-amplitude event on the coherence slice (lighter shades) at 800 ms represents a shallow gas accumulation. Notice that the gas zones form at the intersection of faults trending in orthogonal directions. The arc-shaped fault block on the 1060-ms coherence slice represents the approximate structural configuration of the block. The "wormy" dark zones represent areas of low coherence which often correlate with shale zones of low reflectivity or wipeout zones below shallow gas.

Figures 12e-f are two cross-sectional views through region 3. Both cross-sections show the location of the coherence slices for easy reference. Cross-section A-A′ demonstrates the extensional nature of the north-south faults. The stratigraphic section thickens across each fault block as we move to the east. Cross-section B-B′ exhibits the compressional aspect of the ridge. A horst block resembling an upside down "V" appears on B-B′, starting just below 800 ms. This fault block spreads apart as it proceeds down to 1060 ms and 1200 ms. On the 800-ms coherence slice, the apex of the horst sits close to the intersection of A-A′ and B-B′. The coherence slice at 1060 ms indicates that the fault planes separate by almost a factor of two compared to the previous slice. By 1200 ms, the northern bounding fault of the horst feature starts to bifurcate.

The fault pattern on these coherence slices demonstrates how coherence accelerates interpretation. Interpretation of the intricate details of the complex fault patterns in these slices would require tedious, time-consuming picking. It is very possible that some detail would be overlooked. Coherence, on the other hand, works directly on the data without the interpreter's interaction and thus accelerates the process.

Conclusions. Coherence provides the interpreter with a very powerful tool for delineation of fault trends and identification of stratigraphic and structural features. Comparison between conventional migrated slices and coherence slices shows that the latter extract valuable geologic information from 3-D surveys beyond that on conventional slices. When used in conjunction with seismic cross-sections and other attribute analysis, coherence slices greatly accelerate interpretation of regional geology and geology at the prospect level. Dip/azimuth time slices further augment interpretation by providing information on dip direction and amount of dip of faults and horizons.

Suggestions for further reading. *"3-D seismic attributes using a semblance-based coherence algorithm"* by Marfurt et al., GEOPHYSICS 1998, and *"Eigenstructure-based coherence computations as an aid to 3-D structural and stratigraphic mapping"* by Gersztenkorn and Marfurt, GEOPHYSICS September-October 1999.

Adam Gersztenkorn has worked at Amoco's research facility in Tulsa for the past 15 years. His primary focus during this time was on the research and development of new algorithms for seismic data processing. He received Amoco's 1996 Technology Award for developing the eigenstructure-based coherence algorithm. He is currently a consultant through Geophysical Research and Development (GRAD). He specializes in the development of numerical and computer algorithms for seismic data processing.

Corresponding author: A. Gersztenkorn, adamg3d@aol.com, 1-918-523-8907